EXPERIMENTAL DATA AND CFD PERFORMANCE FOR CLOUD DISPERSION ANALYSIS: THE USP-UPC PROJECT

A. M. Schleder[a], E. Pastor[b,*], E. Planas[b], M. R. Martins[a].

[a]*Analysis, Evaluation and Risk Management Laboratory (LabRisco). Naval Architecture and Ocean Engineering Department, Analysis, evaluation and risk management laboratory, University of Sao Paulo.,Av. Prof. Mello Moraes, 2231, 05538-030 Sao Paulo, Brazil*

[b]*Centre for Technological Risk Studies (CERTEC). Department of Chemical Engineering. Universitat Politècnica de Catalunya · BarcelonaTech. Diagonal 647, 08028 Barcelona, Catalonia, Spain.*
e-mail: elsa.pastor@upc.edu

[*] *Corresponding author: tel: (+34) 934011090, fax: (+34) 934017150; e-mail address: elsa.pastor@upc.edu*

Abstract

Forecasting the behaviour of a flammable or toxic cloud is a critical challenge in quantitative risk analysis. Recent literature shows that empirical and integral models are unable to model complex dispersion scenarios, like those occurring in semi-confined spaces or with the presence of physical barriers. Although CFD simulators are promising tools in this regard, they still need to be fully validated with comprehensive datasets coming from experimental campaigns designed ad-hoc. In this paper, we present an experimental campaign carried out by a joint venture between University of São Paulo and Universitat Politècnica de Catalunya to investigate CFD tools performance when used to analyse clouds dispersion. The experiments consisted on propane cloud dispersion field tests (unobstructed and with the presence of a fence obstructing the flow) of releases up to 0.5 kg/s of 40 s of duration in a discharge area of 700 m^2. We provide a full 1-s averaged propane concentration evolution dataset of two experiments, extracted from 29 points located at different positions within the cloud, with which we have tested FLACS® CFD-software performance. FLACS reproduces successfully the presence of complex geometry, showing realistic concentration decreases due to cloud dispersion obstruction by the existence of a fence. However, simulated clouds have not represented the whole complex accumulation dynamics due to wind variation.

Keywords: consequence analysis, propane, field tests, computational fluid dynamics, FLACS software.

1 INTRODUCTION

Dispersion of hazardous gas releases occurring in transportation or storage installations represent a major threat to health and environment. Therefore, forecasting the behaviour of a flammable or toxic cloud is a critical challenge in quantitative risk analysis. Cloud dispersion is often analysed using Gaussian and integral models that usually provide reliable and fast results for dispersions in simple scenarios, i.e. unobstructed, over flat terrain; however, these models show limitations when applied to study dispersions over terrains with any degree of complexity, like in offshore production units, refineries or industrial plants. Obstacles present in the cloud scattering path interact with the gas flow and generate turbulence causing an important effect in the cloud dispersion. The impact of the geometry on dispersion has to be necessarily evaluated to perform an accurate dispersion analysis and simple models are not able to tackle it. The latter treat terrain complexities by means of a surface roughness parameter, which becomes a very imprecise and unrealistic approximation when modelling dispersion with complex local geometries.

The interest of Computational Fluid Dynamics (CFD) codes to solve complex flow related problems has been extended within the scientific community, together with the increase on computational capacity. One of the areas where CFD has already shown its potential is in risk analysis, and more particularly in dispersion. Although CFD tools spend significantly more time to perform dispersion analysis, they allow taking into account the geometry of elements present in real scenarios, such as barriers or semi-confined spaces. A comparative study between the use of an integral model and a CFD tool to evaluate dispersion analysis is reported by Schleder & Martins (2013a); in this study, a LNG (liquefied natural gas) leakage in a semi-confined space was simulated using the UDM (unified disperision model (Haper, 2009) model and the FLACS CFD-simulation tool (GexCon AS, 2013), showing the latter the ability to realistically peak the concentration variations due to the presence of an obstacle placed at the dispersion path, which led to an increase of the LFL (lower flammability limit) distance reached by the vapour cloud. Sklavounos & Rigas (2006) compared the performance of the

CFD code CFX(Ansys Inc., 2011) with two traditional models –SLAB (Ermak, 1990) and DEGADIS (Reynolds, 1992) – when challenged to simulate also an experimental LNG release. Their results showed that the CFD code presented better accuracy than the integral models when reproducing concentration distributions in the dispersion field.

In recent years the use of CFD tools to perform dispersion analyses has been increased and although they have been proven promising, they still present some challenges to overcome. As shown by Plasmans et al. (2012), large differences may arise among simulation results when using different CFD tools and/or different CFD analysts to assess the same dispersion scenario. In CFD simulations, a wide range of computational parameters must be set by the user, which may affect the results significantly. For instance, in a typical simulation the user must select the variables of interest, has to be able to choose a turbulence model from a set of available options, must define the computational domain and mesh, must specify the boundary conditions, the methods of discretization and the convergence criteria, among others. Sensitivity tests and validation studies have been conducted during the last years in order to provide insights on how to appropriately set CFD simulations (e.g. Sklavounos and Rigas, 2006; Cormier et al., 2009; Tauseef et al., 2011), but to do that, reliable experimental data is needed. There are few reported field experiments in the literature dealing with dispersion and even less dealing with dispersion in environments with some degree of complexity. The majority of these tests were performed decades ago, and the data generated is not comprehensive enough for an exhaustive evaluation of CFD tools performance.

1.1 Literature review on dispersion experiments

Most of the field tests performed in the past involved LNG dispersions, since during the decades of 70 and 80 a huge effort was conducted in order to fully understand the behaviour of LNG when released accidentally (e.g. Blackmore, Eyre and Summers 1982; Koopman et al., 1982; Goldwire et al., 1983). More recently, experiments involving LNG releases on water have been performed (Hanlin, 2006). Field tests involving other substances such hydrogen or tracer gases are found in smaller proportion (Middha & Hansen, 2009; Biltoft, 2001; Allwine and Flaherty, 2007), although the tests involving the former substance have been increased in last years.

Among the more classical dispersion field tests used for validation purposes, the Falcon and the Burro series (reported by Koopman et al. 1982 and Brown et al. 1990, respectively) have to be highlighted. Both tests consisted of LNG spills; the Burro tests were undertaken at an open area without obstacles whereas the Falcon tests were performed in a terrain with obstacles. These tests have been extensively used for models validation (e.g. Ermak, Chan, Morgan, & Morris, 1982; Gavelli, Bullister, & Kytoma, 2008; Hansen, Gavelli, Ichard, & Davis, 2010). However, it is important to note that the tests were made decades ago, when the range of measurement and data logging equipment was not as comprehensive as nowadays and therefore data available from these tests is scarce for an overall CFD validation exercise.

Later on, Gaz de France and Associates (Butler and Royle, 2001) conducted experiments involving the dispersion of a dense gas in an environment with obstacles. However, the project was focused on flash fires and not on cloud dispersion. In most trials, the cloud was ignited few seconds after the gas release started and therefore, it hardly dispersed. Still in the 2000 first decade, the tests MUST (Biltoft, 2001), MID05 (Allwine and Flaherty, 2007) and MKOPSC (Cormier et al., 2009) were carried using tracer gas (the first two) and LNG as substances. They were undertaken by a consortia involving private companies; therefore, only a small portion of the collected data is publicly available through published reports, which hampers its use to perform validation studies. More recently, in 2010, the Jack Rabbit test was conducted in order to assess the behaviour of a cloud generated by a large amount of ammonia released instantaneously in a terrain depression, and although it is rated as a test with obstructions, its scenario is very restricted since the obstruction is just the result of the changing slope in the terrain (Hanna et al., 2012). It is worth to note that most published data only contain values of peak concentrations or concentrations in a specific moment after the release. Concentration evolution with time and space can be hardly found in the literature which reduces the possibility to explore CFD validity for dispersion studies.

1.2 The USP-UPC Project

As the literature review shows, there is a lack of complete experimental data to assess the use of CFD tools for consequences analysis involving dispersion of flammable and toxic substances. To overcome this drawback, a joint venture between University of São Paulo (USP) and Universitat Politècnica de Catalunya (UPC) has recently been established to investigate the performance of CFD tools when analysing cloud dispersion of flammable/toxic substances by means of ad-hoc experimentation.

The first stage of the experiments planned in this project was undertaken at Can Padró Security and Safety training site during 22nd-25th July of 2014 and consisted of LPG clouds formation and dispersion tracking. Eleven trials were performed, comprising a total amount of around 70 kg of LPG emitted. The vapour clouds were intensively monitored to determine concentration evolution with time and space.

The paper at hand provides a description of this first USP-UPC campaign and gives details of the experimental data of two of the trials and their simulation using FLACS simulation software, which is a CFD tool specifically developed for consequence analysis. The objectives of this paper are to offer new sets of experimental cloud dispersion data to the international community and to show preliminary results of CFD performance to simulate two of the experiments, as an example of the potential uses of the data gathered during the tests.

2 EXPERIMENTAL SET-UP

The field tests consisted of continuous releases of LPG in the atmosphere with the subsequent resulting cloud formation. LPG composition consists of 97% propane (volume), 1.5% butane and 1.5% of other gases such as hydrogen and nitrogen. Experiments were intensively monitored and concentration was characterized as a function of time and space. The LPG was stored in a 4 m^3 pressurized vessel (saturation pressure at ambient temperature) located roughly 45 m apart from the cloud dispersion path on an upper site, at a relative elevation from the ground of 15 m. The fuel flowed through a 40 mm diameter pipe with a total length of 50 m down to the release point, which was located at 1.5 m high (Figure 1).

Pressure and temperature were monitored at the release point by an electronic pressure transmitter (Barksdale, type UPA5) and two K-type thermocouples located 0.05 m upstream of the outlet orifice,

both recording at a frequency of 4 Hz. This data was used to calculate the mass flow rate ant the jet velocity at the outlet orifice assuming isentropic expansion between the stagnation point and the orifice jet exit, by applying the appropriate thermodynamic relationships.

Additionally, sensors were deployed over a 700 m^2 area (35 m in release direction and 20 m in cross direction). 47 self-powered electrochemical oxygen sensors (2FO flue gas sensor of CiTicel) were placed at 19 different locations within the discharge area at three different heights: 0.1, 0.6 and 1.3 m (Figure 2). We choose this type of sensors as an indirect measure of LPG concentration, since we assumed that any decrease in the concentration of oxygen was caused by displacement of oxygen by the LPG vapour. Oxygen sensors were made of a galvanic cell, being the current flow between the cell electrodes proportional to the oxygen concentration to be measured. The sensors contained a bridge resistor to provide a voltage power (mV) output. A small amount of oxygen was consumed in the cell reaction in order to produce the current flow and the subsequent voltage power output. Assuming an atmospheric oxygen concentration of 20.9% (volume) and an atmospheric nitrogen concentration of 79.1% , the LPG vapour concentration $[LPG_v]$ could then be expressed as:

$$[LPG_v] = 1 - [O_2] - \frac{79{,}1[O_2]}{20{,}9}$$

Being $[O_2]$ the oxygen concentration detected by the sensors.

Some of the experiments were designed to investigate the influence of an obstruction placed in the dispersion path; thus, in some trials a 1.3 m-height 1 m-width fence was placed perpendicular to the jet direction at the centreline of the sensors array 10 m apart from the release point.

Furthermore, 1 meteorological station (Vantage Vue Wireless of Davis Instruments) and 5 ultrasonic wind sensors (WindSonic OP1 of Gill Instruments) were used to monitor the weather conditions. Wind direction and speed measurements were made at a frequency of 1 Hz; the wind sensors were placed at 1 m height at position W1A and at 1 m and 2 m height at positions W2AB and W3AB (see Figure 2). Ambient temperature and relative humidity was obtained by means of the meteorological station located at the site.

In order to register and store the sensors data, one datalogger model DT85 of DataTaker Loggers, with 2 expansion modules CEM20 and one data acquisition system model Field Point of the National instruments were used. The data were recorded at a rate of 4 hertz.

Eleven trials were taken with different releases rates and spill durations. In the present paper only two of these trials are presented and intensively discussed: P25_2 and P25_3. These trials were chosen due to the similarity of initial conditions: the former consisted of a release of 8 kg with no obstacles and the second consisted of a release of 6 kg in the presence of the fence, both releases with 40 s duration. Figure 3 shows an instant of trial P25_2. It can be observed the release point, several masts used to sustain the temperature and oxygen sensors (positions 1, 2, 3, 4, 5, 8 and 10 as detailed in Figure 2) the 3 higher masts (positions W1, W2 and W3) used to support the anemometers and the vapour cloud formed.

3 CFD MODELLING

The CFD simulations were performed using FLACS® software (GexCon). FLACS is a CFD tool that was specifically developed for consequence modelling. It uses conservation equations for mass, energy, and momentum; it solves Reynolds Averaged Navier-Stokes (RANS) equations based on the standard k-ε turbulence model of Launder & Spalding (1974). According to HSE (2013), RANS approach is widely accepted in engineering CFD studies; it is based on the concept of separating the fluid velocity components and scalar quantities (pressure, temperature, concentration) into mean and fluctuating components, then transport equations are used to evaluate the model. The model of Launder & Spalding (1974) is based on the turbulent kinetic energy and its dissipation rate; the magnitudes of these two variables are calculated from transport equations and solved simultaneously with those governing the mean flow behaviour.

3.1 Physical settings of the scenarios

CFD simulations of trials P25_2 and P25_3 were performed to challenge FLACS against the experimental data. The scenario conditions used to perform the simulations are presented in Table 1. Values of ambient temperature, ambient pressure, relative humidity and wind direction and speed were

considered as the median of the recorded values during the duration of each test. In a previous sensitivity analysis reported elsewhere (Schleder, 2015) we found that environmental variables did not show high sensitivity scores, so that we relied on the experimental measurements to set our simulations. The ground roughness was assumed equal to 0.03, which is the typical value for concrete surfaces (GexCon AS, 2013). The Pasquill class used was E – slightly stable. At the moment of the trials, there was a cloud cover of around 80% and it had been raining during 2 hours prior to the beginning of the tests. This condition reduced considerably the heat emitted from the ground leading to stable atmospheric condition.

The pressure and temperature ranges at the outlet orifice are detailed on Table 1 by the minimum and the maximum values registered during the duration of the trials. 1s averages of the measured temperature and pressure values were used to calculate the release rate. As previously mentioned, the jet velocity at the outlet orifice and the mass flow rate were calculated assuming isentropic expansion between the stagnation point and the orifice jet exit; the total amount of fuel released was obtained by the integral of the mass flow rate during the release. The simulations were performed by considering a 1 second-averaged variable mass flow rate.

Table 1 - Scenario conditions

Variable	**Unit**	**P25_2**	**P25_3**
Ambient Temperature	°C	21.2	22.5
Ambient pressure	hPa	993	993
Relativity humidity	%	86.8	86.9
Wind direction	°	185	235
Wind speed at 1 m high	$m \cdot s^{-1}$	0.49	0.70
Pasquill Class	-	E	E
Ground roughness	m	0.03	0.03
Discharge direction	-	horizontal	horizontal
Discharge height	m	1.5	1.5
Release duration	s	40	40
Temperature release range (min/max)	°C	-28.1/4.7	-28.41/10.26
Pressure release range (min/max)	bar	0.1/1.2	0.1/1.3
Amount of fuel released	kg	8.0	6.5
Discharge rate (min/max)	$kg \cdot s^{-1}$	0.04/0.38	0.08/0.39

3.2 Domain and grid definition

The simulation domain was discretized using a single block Cartesian grid, defined following FLACS user manual guidelines (GexCon AS, 2013). An orthogonal base X, Y and Z was used, being X horizontal and parallel to the jet direction, Y horizontal and perpendicular to the jet direction and Z vertical. The domain extended 50 m in the X direction (from 5 m before the release point to 45 m after the release point), 48 m in the Y direction (centred on the release point) and 10 m in the Z direction (from de ground level). As such, the release point coordinate was (0, 0, 1.5) in our domain. The domain was defined using two types of meshes (Figure 4a): the former being a coarse (macro) grid, representing the zone where the dispersion is expected to occur; and the latter being a fine (micro) grid, representing two different swaths intersecting around the release point: one vertical, formed by a mesh of cells at the centreline of the dispersion path, and the other horizontal, formed by a mesh of cells centred at 1.5 m height (i.e. release height).

The cells were represented by 1 m edge cubes at the macro grid. In order to set the micro grid we followed the FLACS guidelines (GexCon AS, 2013); which specifies that the area of the expanded jet (A_{jet}) must be solved in only one cell and that the area of this cell across the jet (A_{cv}) should be larger than the area of the expanded jet but not larger than twice A_{jet} (Figure 4b). The jet area expected after the expansion at ambient pressure was estimated using the FLACS jet utility –which is based on a one-dimensional model for the release of an ideal gas from a pressurized reservoir through a nozzle into an open atmosphere (GexCon AS,2013)– and the dimensions of the cell across the jet were defined so that the area fell between the specified limits. Thus, the width and height of the micro grid cells were fixed at 0.04 m (as a function of the jet area expected after the expansion at ambient pressure).

The FLACS guidelines also recommend that the aspect ratio (the ratio between the smallest and largest side of the cell) of the micro grid has to be not larger than five (due to stability of the numerical solution); thus, the length of the cells was fixed at 0.20 m. Next, the cells nearby the leak were smoothly increased to the macro grid resolution (see Figure 4a), maintaining the maximum change in

grid resolution from one grid cell to the next one less than 40% (as recommended by the FLACS guidelines).

Finally, monitoring points were inserted in the simulation specifications at the same locations where the sensors were placed in the field, which allowed the measured values of concentration and temperature to be compared with the simulated values.

4 RESULTS AND DISCUSSION

As previously mentioned, one of the aims of this study is to offer new sets of cloud dispersion data to the international community to: i) be used for models validation studies and to ii) provide new insights of gas dispersion phenomena in realistic environments. The most relevant data acquired during P25_2 and P25_3 tests are presented in this section and more detailed information is included in annex A (i.e. LPG release rates and concentration evolutions with time and space). It has to be said that it had been raining during 2 hours prior to the beginning of the tests and some sensors did not work well due to accumulated water over the sensor output.

Another aim of this study was to investigate at an initial stage the CFD performance when challenged to reproduce cloud dispersion in complex scenarios. To address this objective concentration was defined as the main variable of interest.

4.1 Trial P25_2

Figure 5 a) shows experimental versus simulated values of peak LPG concentrations calculated from 12 active oxygen concentration sensors at the centreline during trial P25_2. The experimental data fits within a range of 0.01% - 7.43% of LPG. As expected, the highest concentrations were measured in the first 5 m from the release point in the area where the jet was expected.

The CFD performance when challenged to simulate P25_2 experimental scenario was evaluated using the factor of two (FAC2) range, which analyses whether the simulated values fall within a ±factor of two of the measured data. This factor is widely used for CFD validation purposes. It was one of the parameters recommended by Weil et al. (1992) and Hanna et al. (2004) to evaluate air quality models, later on, it was recommended by HSE in the Model Evaluation Protocol (Ivings et al. 2007) and more

recently it was used by Coldrick et al. (2009) and Ivings et al. (2013). It has to be also noted that the authors have already applied this criterion in previous studies (Schleder & Martins, 2013, Schleder et al. 2014). FAC2 confidence limits are included in the previous figure as dashed lines. 75% of the plotted points fit within this range.

In Figure 5 a), it can be observed how only three points did not adjust to the FAC2 range. Two of them were representing the concentrations measured by two sensors placed 2 m apart from the release point at 0.1 and 0.6 m high, respectively. In those locations, the simulated values (both <0.1%) were significantly lower than the measured concentration real sensors (0.3 % and 2.2% respectively). These two points are the ones with their respective symbols fully stepping on the abscissa axis. The third sensor was placed 5 m from the release point at 0.6 high. The simulator also failed when trying to predict the maximum LPG concentration at a point (5, 0, 0.6), since the simulated value (0.3%) was significantly lower than the measured concentration (1.28%).

The same FAC2 analysis was performed considering all the sensors that worked well during the tests (Figure 5 b)), not just those located at the centreline. Compared to Figure 5 a), the agreement was poorer, with 60% of the plotted points within the FAC2 range. The simulator had bigger errors when simulating concentrations out of the dispersion path axis, where turbulence may have bigger effects; 5 out of 10 concentration values located at the left hand side of the dispersion path following the jet direction (2 m of displacement in y direction), and 4 out of 7 values located at the right hand side (also 2 m displaced) fell out of the FAC2 limits, showing a clear underestimation tendency

4.1.1 Concentration dynamics with time of trial P25_2

Concerning the evolution of the concentration with time, FLACS was able to peak the general trend for most of the sensors, excepting those placed near the source term (in the first 5 m of the discharge path) in which the simulator underestimated significantly the measured values, as previously noted. Figure 6 and Figure 7 show two examples of the LPG comparison of the real/simulated concentration evolution with time plotted for two oxygen concentration sensors, the first located at the centreline 9 m apart from the release point (sensor 6A at a height of 0.1 m) and the other located 15 m apart from

the release point, at the centreline too (sensor 16B, at a height of 0.6 m). Measured release rate (which acts also as input in the FLACS scenario) is also plotted for comparison purposes.

Regarding the sensor 6A, it can be observed how simulated concentration is more sensitive to release rate changes than the real concentration. As such, an initial peak (simulated, 1.3%) can be found around 5 s, which is the response of a maximum release rate occurring roughly one second before. The real concentration evolution is smoother, nevertheless showing also a peak (of around 1%) one second later than the simulated one. This tendency can still be observed when paying attention to the release rate drop occurring 14 s after the start of the test: simulated concentration reacts accordingly showing a drop 5 seconds after, whereas the real concentration takes longer to descend, showing a minimum 8 seconds after the release rate drop. Certainly, there is an increasing delay between the dynamics of the simulated cloud and the real one, and as such the simulated cloud dilutes faster than the real one. This is due to the fact that the simulated cloud is not able to pick the accumulation that the real one experienced. This becomes more evident 25 seconds after the start of the release, when real concentration in sensor 6A increases, while the simulated one decreases according to the pattern shown by the release rate evolution. Furthermore, it is also possible to note greater oscillations on the measured concentration values compared to the predicted values.

Sensor 16 B behaves in a similar way: although the first concentration maximum is accurately picked by the simulated cloud (both in terms of absolute value and instant of time), the simulated cloud disperses faster, not showing the accumulation registered by the real sensor. Also, simulated concentration curve is smoother compared to the real evolution.

One of the reasons that could explain these particular lacks of accuracy could be found in the simulated wind. A constant wind is considered in the simulations, which gives reasonably good results when simulating concentration in the centreline (note that variations of ±20% of mean wind speed did not increase the simulator performance -data not shown). However, FLACS loses accuracy when simulating concentrations at location out of the dispersion path axis. During the execution of the test, there were oscillations on wind speed and direction, the wind speed ranged between 0.03 $m \cdot s^{-1}$ and 1.02 $m \cdot s^{-1}$ and the direction between 63º and 287º. With a simulated wind dynamics simpler than the real one, FLACS may represent less turbulent eddies than the real ones occurring in the experimental

site. Therefore, the simulated cloud disperses smoothly than the experimental cloud. However, in order to verify this hypothesis more experimental data covering a wider range of wind conditions would be needed as well as better representation of wind profile in the simulations.

4.2 Trial P25_3

Figure 8 a) presents measured versus simulated values of peak LPG concentrations at the centreline calculated from 12 active oxygen concentration sensors during the trail P25_3. The trial P25_3 was undertaken some minutes after trial P25_2; thus, the values in Figure 8 correspond to the same sensors of the centreline that did work well during trial P25_2.

In this case, 83% of the predicted/measured points also fit well within the range of factor2. As in the previous trial, for the two sensors placed 2 m apart from the release point, at 0.1 and 0.6 m high, no significant concentrations were predicted.

In addition, performing the same FAC 2 analysis considering all the sensors (not just those located at the centreline), 70% of the points were found to fit well within the FAC 2 range. Similarly to trial P25_2, the agreement decreased when adding concentration values measured out of the dispersion path axis. In this case, however, the simulator bias did not show a clear tendency, presenting over/underestimated values in similar proportion.

4.2.1 Concentration dynamics with time of trial P25_3

Figure 9 and Figure 10 show two examples of the LPG concentration evolution with time calculated from two oxygen concentration sensors, one located at the centreline, 1 m after the fence (0.6 m high, sensor 11B) and the other, located at the same place, but at a height of 1.3 m (sensor 11C). Concerning sensor 11B, it can be seen how both concentration curves, measured and simulated, present a very good agreement. It is worth noting that there is a time delay (of around 4 s) when comparing predicted vs. measured peak concentrations, but in this case the first maximum is the one corresponding to the measured concentration. Despite this initial delay, however, the simulated cloud again seems to dilute faster than the real one. The effect of the fence can be clearly observed in both real and simulated curves; although the release rate keeps around 0.15-0.2 $kg.s^{-1}$ during the last period of the experiment

(between 28 s – 38 s), concentration values show a general decreasing trend. Again, it can be clearly seen how the simulated curve is smoother than the real one, for the above mentioned reasons. Concentration evolution of sensor 11C is rather well simulated too. In this case, the simulated cloud shows a maximum peak in the 11C sensor location faster than the real one. However, the simulated cloud dilutes faster. Interestingly, the simulated cloud fails to represent the complex accumulation dynamics detected by the real sensor occurring from 30 seconds after the release. Rather, simulated concentration becomes negligible during this particular period.

4.3 Cloud concentration profiles

Figure 11 and Figure 12 show the cloud concentration profile at the centre plane of the cloud path (Y=0) 10 s after the release start, for trials P25_2 and P25_3 respectively. Some monitor points with their related concentrations (experimental and simulated) are gathered in the box. In monitoring points of Figure 11, the mean error between measured and simulated values was 13%. It is worth noting that, at this instant, concentrations were low and although maximum errors of around 39% were found (e.g. error in 11C), they do not represent large discrepancies, e.g. the maximum difference between the simulated and the measured volumetric concentration is only of 0.41% (sensor 11C).

Concerning to trial P25_3 (Figure 12) the mean error between simulated and experimental concentration was 18%, with a maximum error of 36% when simulating the concentration of the sensor 16B (errors roughly of the same order of magnitude than ones computed for the trial P25_2). Moreover, it is possible to verify the influence of the fence placed 10 m apart from the release point on the cloud dispersion, since part of the cloud is trapped before the barrier. In P25_3, the simulated propane concentration at locations 11B, 11C, 16A and 16B were significantly lower than the concentrations simulated at the same positions for trial P25_2, with decreases between 13% and 44%.

5 CONCLUSIONS AND FUTURE WORK

This paper presented the first stage of the experimental campaign undertaken by the joint venture between University of São Paulo and Universitat Politècnica de Catalunya envisaged to provide

experimental data about gas dispersion with the aim of investigating the performance of CFD tools for cloud dispersion of flammable/toxic substances modelling.

The literature review show evidence that data on concentration of toxic or flammable clouds as a function of time and space are very scarce. Usually the experimental data is presented in graphs of concentrations at specific instants and positions, and in most cases, only peak values are provided. The data provided here is much comprehensive than any other published experimental dataset concerning cloud dispersion, which will be particularly suitable for the scientific community to perform complete models validation and comparison studies, and conduct time dependent analysis of cloud dispersion behaviour.

The tests performed by USP-UPC consisted of continuous LPG releases at the atmosphere and the subsequent monitoring and characterization of the cloud concentration and temperature. Some of the trials undertaken were designed to investigate the influence of an obstruction placed in the path of the vapour flow. We provide comprehensive LPG concentration data of two particular tests: trials P25_2 and P25_3. These trials are similar in release conditions; however, the former is a release without obstacles and the second has an obstruction 10 m apart from the release point.

Some preliminary analysis comparing LPG concentration data of these two tests with CFD simulations were presented. In general terms, the CFD-based simulator has shown good performance when simulating cloud concentration. It has to be highlighted that FLACS passes with good accuracy the FAC2 test, which is a well-established and standardized indicator for model validation purposes. FLACS shows mean errors of 13% for unobstructed scenarios, and of 18% for obstructed ones, which are acceptable given the general dynamics of the experimental tests (i.e. unsteady release rate and wind fluctuations in speed and direction). Moreover, FLACS seems to successfully reproduce the presence of complex geometry and its effects on cloud dispersion, showing realistic concentration decreases due to cloud dispersion obstruction by the existence of a fence.

FLACS performance may be improved by setting the scenario considering more complex wind dynamics as the ones encountered during the field tests, at the expense, however, of the simulation runtime. To the best of our knowledge, a variable wind profile in CFD simulations has never been

considered for dispersion analysis, however real scenarios are far from having stable wind. This is surely a relevant point which shall be explored in our future work.

ACKNOWLEDGEMENTS

The authors gratefully wish to acknowledge the personnel of Can Padró Security and Safety Training site as well as the UPC research scientists Diana Tarragó, Oriol Rios and Miguel Muñoz for their help and expertise during the design and performance of the field tests.

This paper reports part of the overall results obtained in the R&D project grant 2013/18218-2 sponsored by São Paulo Research Foundation (FAPESP), whose support the authors gratefully wish to acknowledge. The authors also gratefully wish to acknowledge the Program for Development of Human Resources (PRH19) from Petrobras and Brazilian National Petroleum, Natural Gas and Biofuels Agency (ANP) by the financial support, and also thank the Spanish Ministerio de Ciencia e Innovación (projects CTQ2011-27285 and CTM2014-57448-R) and the Autonomous Government of Catalonia (project no. 2014 SGR 0413) for sponsoring this research.

REFERENCES

Allwine, K. J., & Flaherty, J. E. (2007). *Urban Dispersion Program Overview - PNNL-16696.* Pacific Northwest National Laboratory, Richland, US.

Ansys Inc. (2011). *ANSYS CFX Theory Guide.* Canonsburg.

Biltoft, C. A. (2001). *Customer Report for Mock Urban Setting Test (MUST). DPG Doc. No. WDTC-FR-01-121.* West Desert Test Center, U.S. Army Dugway Proving Ground, Dugway, UT 84022-5000.

Blackmore, D. R., Eyre, J. A., & Summers, G. G. (1982, May 10). Dispersion and combustlon behauiour of gas clouds resulting from large spillages of LNG and LPG on to the sea. *The institute of marine engineers, 94*(29), pp. 1-18.

Brown, T. C., Cerdewall, R. T., Chan, S. T., Ermak, D. L., Koopman, R. P., Lamson, K. C., et al. (1990). *Falcon series data report: 1987 LNG vapor barrier verification field.* Research Institute, Report nº GRI-89/0138.

Butler, C. J., & Royle, M. (2001). *Experimental data acquistion for validation of a new vapour cloud fire (VCF) modelling approach.* 1-102: Health and Safety Laboratory - HSE.

Coldrick, S., Lea, C. J., & Ivings, M. J. (2009). *Validation database for evaluating vapor dispersion model for safety analysis of LNG facilities - Review.* The fire protection research foundation.

Cormier, B. R., Ruifeng, Q., Yun, G., Zhang, Y., & Mannan, M. S. (2009). Application of computational fluid dynamics for LNG vapor dispersion modeling: A study of key parameters. *Journal of Loss Prevention in the Process Industries*, pp. 332-352.

Ermak, D. L. (1990). *User's manual for SLAB: an atmospheric dispersion model for denser-than-air.* California: Lawrence Livermore National Laboratory.

Ermak, D. L., Chan, S. T., Morgan, D. L., & Morris, L. k. (1982). A comparison of dense gas dispersion model simulations with Burro series LNG spill test results. *Middha & Hansen, 2009), 6*, pp. 129-160.

Gavelli, F., Bullister, E., & Kytoma, H. (2008). Application of CFD (Fluent) to LNG spills into geometrically complex environments. *Journal of Hazardous Materials 159*, pp. 158-168.

GexCon AS. (2013). *FLACS v10.0 User´s Manual.* Norway.

Goldwire, H. C., Cederwall, R. T., Rodean, H. C., Kansa, E. J., Koopman, R. P., McClure, J., et al. (1983). *Coyote Series Data Report, LLNL/NWC - LNG Spill Tests Dispersion, Vapor burn and rapid-phase transition.* Livermore, California: vols. 1 and 2, UCID-19953 Lawrence Livermore National Laboratory.

Hanlin, A. L. (2006). A review of large-scale LNG spills: Experiments and modeling. *Journal of Hazardous Materials, A132*, pp. 119-140.

Hanna, S. R., Hansen, O. R., & Dharmavaram, S. (2004). FLACS CFD air quality model performance evaluation with Kit Fox, MUST, Praire Grass, and EMU observations. *Atmospheric Enviroment, 38*, pp. 4675-4687.

Hanna, S., Britter, R., Argenta, E., & Chang, J. (2012). The Jack Rabbit chlorine release experiments: Implications of dense gas removal from a depression and downwind concentrations. *Journal of Hazardous Materials*(212), pp. 406-412.

Hansen, O. R., Gavelli, f., Ichard, M., & Davis, S. G. (2010). Validation of FLACS against experimental data sets from the model evaluation database for LNG vapor dispersion. *Journal of Loss Prevention in the Process Industries*, pp. 857-877.

Haper, M. (2009). *UDM Theory Document.* London, UK: DNV Softaware.

HSE-Health and Safety Executive. (2013). *Fire and Explosion Strategy - Issue 1.* Hazardous Installations directorate - Offshore division.

Ivings, M. J., Lea, C. j., Lea, C. J., & Webber, D. M. (2007). *Evaluating vapor dispersion models for safety analysis of LNG facilities.* The fire protection research foundation.

Ivings, M. J., Lea, C. J., Webber, D. M., Jagger, S. F., & Coldrick, S. (2013). A protocol for the evaluation of LNG vapour dispersion models. *Journal of Loss Prevention in the Process Industries*(26), pp. 153-163.

Koopman, R. P., Cerdewall, R. T., Ermak, D. L., Goldwire, H. C., Hogan, W. J., McClure, J. W., et al. (1982). Analysis of Burro series 40m3 LNG spills experiments. *Journal of Hazard Materials, 6*, pp. 43-88.

Launder, B. E., & Spalding, D. B. (1974). The numerical computation of turbulent flows., *3*, pp. 269-289.

Middha, P., & Hansen, O. R. (2009). Using computational fluid dynamics as a tool for hydrogen safety studies. *Journal of Loss Prevention in the Process Industries, 22*, pp. 295-302.

Plasmans, J., Donnat, L., de Carvalho, E., & Debelle, T. (2012). Challenges with the use of CFD for major accident dispersion modeling. *Process Safety Progress, 32*, pp. 1-8.

Reynolds, M. R. (1992). *ALOHA (Areal Locations of Hazardous Atmospheres) 5.0 Thoretical description.* Washington: NOAA Technical Memorandum NOS ORCA-65.

Schleder, A.M. (2015). Quantitative dispersion analysis of leakages of flammable and/or toxic substances on environments with barriers or semi-confined. PhD dissertation. Universidade de Sao Paulo - Universitat Politècnica de Catalunya, 184 pp.

Schleder, A. M., & Martins, M. R. (2013). The use of Integrals and CFD tools to evaluate the cloud dispersion of flammable and toxic substances leakages. *Proceedings of ESREL 2013 - European Safety and Reliability Con-gress*, (pp. 1-8). Amsterdam.

Schleder, A. M., & Martins, M. R. (2013a). Comparative evaluation of the cloud dispersion of a liquefied natural gas leakage using the UDM and a CFD model. *Proceedings of the ASME 2013 32th International Conference on Ocean, Offshore and Arctic Engineering - OMAE2013*, (pp. 1-8). Nantes.

Schleder, A. M., Martins, M. R., Pastor, E., & Planas, E. (2014). The effect of the computational grid size on the prediction of a flammable cloud dispersion. *Proceedings of the ASME 2014 33th International Conference on Ocean, Offshore and Arctic Engineering - OMAE2014*, (pp. 1-9). San Francisco.

Sklavounos, S., & Rigas, F. (2006). Simulation of Coyote series trials—Part I: CFD estimation of non-isothermal LNG releases and comparison with box-model predictions. *Chemical Engineering Science, 61*, pp. 1434-1443.

Tauseef, S. M., Rashtchian, D., & Abbasi, S. A. (2011). CFD-based simulation of dense gas dispersion in presence of obstacles. *Journal of Loss Prevention in the Process Industries, 24*, pp. 371-376.

Weil, J. C., Sykes, R. I., & Venkatram, A. (1992). Evaluating Air-Quality Models: Review and Outlook. *Journal of Applied Meterorology, 31*, pp. 1121-1145.

FIGURE CAPTIONS

Figure 1. Layout of the propane installation

Figure 2. Oxygen sensor array (blue points); the numbers are identifiers of the masts were the sensors were attached and the letters A, B and C represent the sensors height, at 0.1 m, 0.6 m and 1.3 m respectively. (e.g. the mast "3ABC", located at the centreline of the dispersion path 5 m apart from the release point, sustained sensors at three heights: 0.1 m, 0.6 m and 1.3 m). The yellow points named W1-W3, represent the location of the anemometers at 1 m height (A) and 2 m height (B).

Figure 3. Photo of trial P25_2, showing the release point and masts; at 40 s from the beginning of the release and release rate of 0.17 kg/s.

Figure 4. a) Grid representation; b) micro grid cell containing the release point. A_{jet} is the jet area expected after the expansion at ambient pressure and A_{cv} is the area of the cell across the jet. For both areas, the following relation must be fulfilled: $Ajet < Acv < 2 \cdot Ajet$

Figure 5. Comparison between simulated peak concentration and experimental data of a) centreline monitored points b) all monitored points of trial P 25_2

Figure 6. Measured and simulated concentrations at sensor 6A position, in the centreline, 9 m from the release point 0.1 m high.

Figure 7. Measured and simulated concentrations at sensor 16B position, in the centreline, 15 m from the release point 0.6 m high.

Figure 8. Comparison between simulated values and experimental data of a) centreline monitored points b) all monitored points of trial P 25_3.

Figure 9. Measured and simulated concentrations at sensor 11B position in trial P25_3 (1 m after the fence at 0.6 m high).

Figure 10. Measured and simulated concentrations at sensor 11C position in trial P25_3 (1 m after the fence at 1.3 m high).

Figure 11. Cloud profile concentration of Trial P25_2 at centreline, 10 s after the release start.

Figure 12. Cloud profile concentration of Trial P25_3 at centreline, 10 s after the release start.

FIGURES

Figure 1

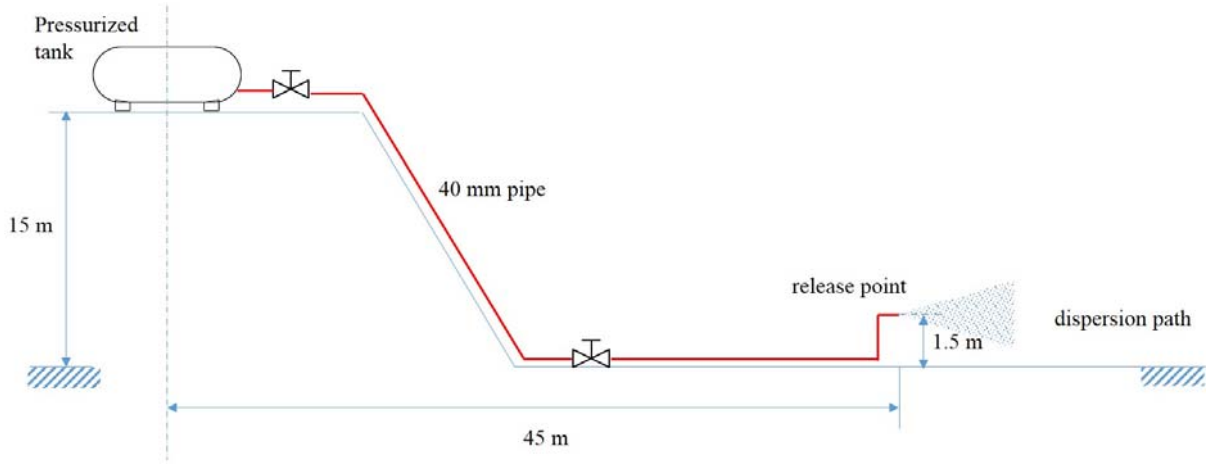

Figure 2

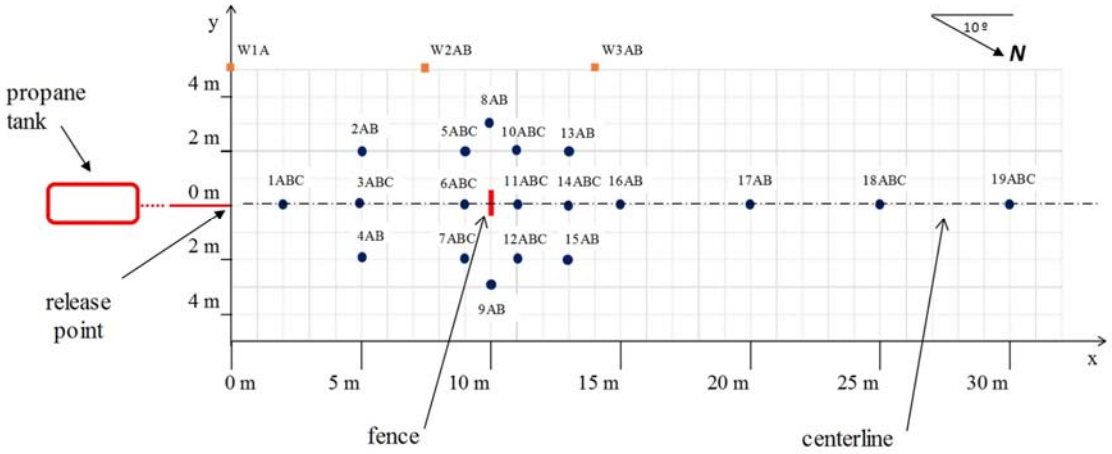

Figure 3

Figure 4

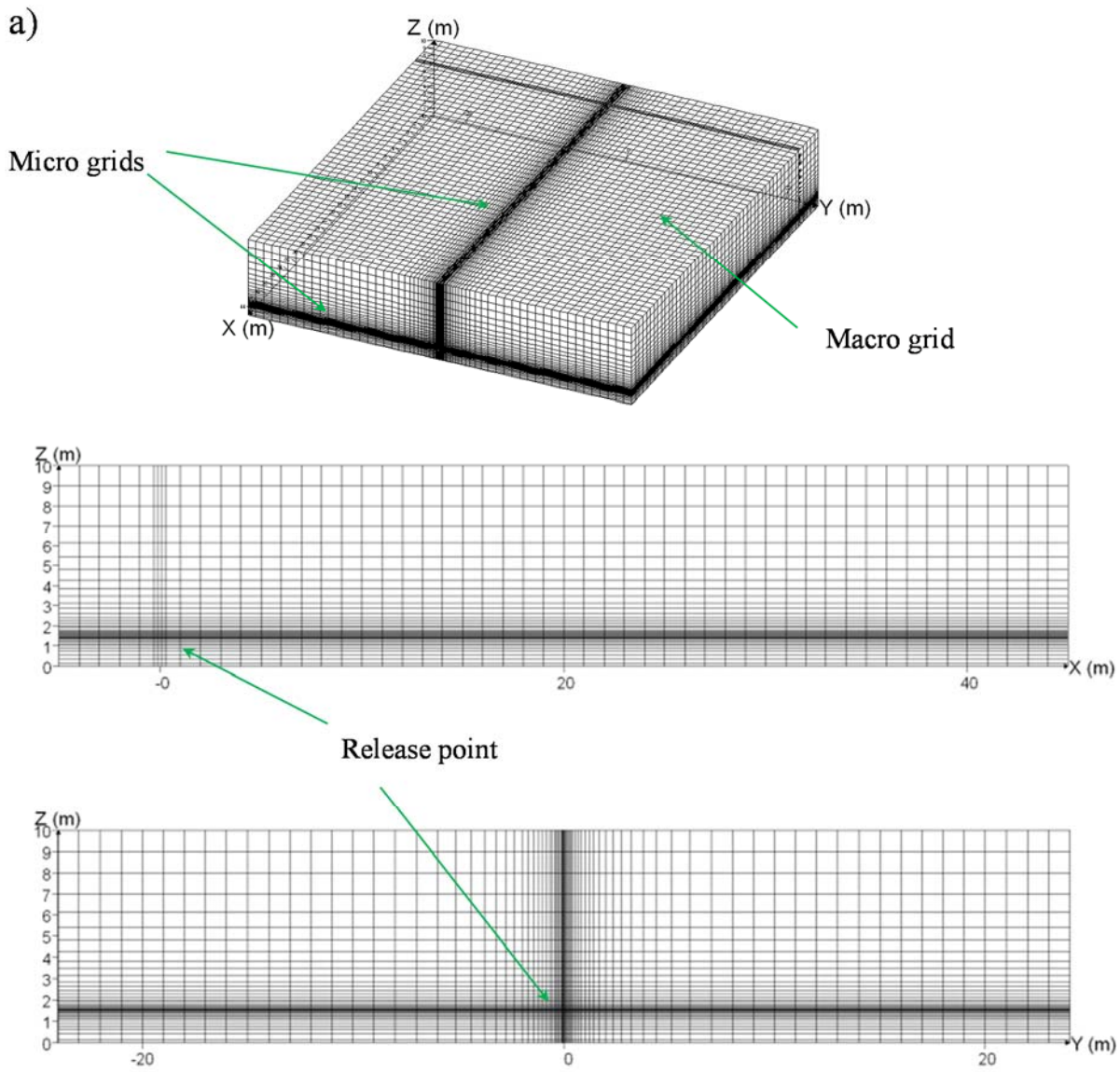
a)
Z (m)
Micro grids
Y (m)
X (m)
Macro grid
Z (m)
X (m)
Release point
Z (m)
Y (m)
b)
A_{cv}
A_{jet}
0.04 m
Release point
0.2 m

Figure 5

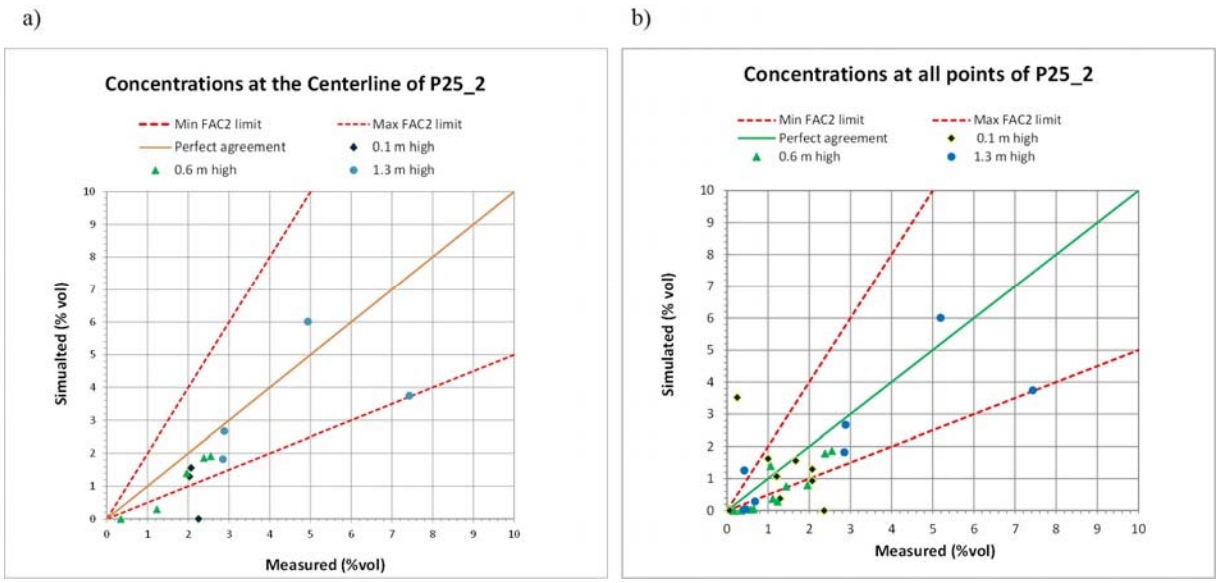

Figure 6

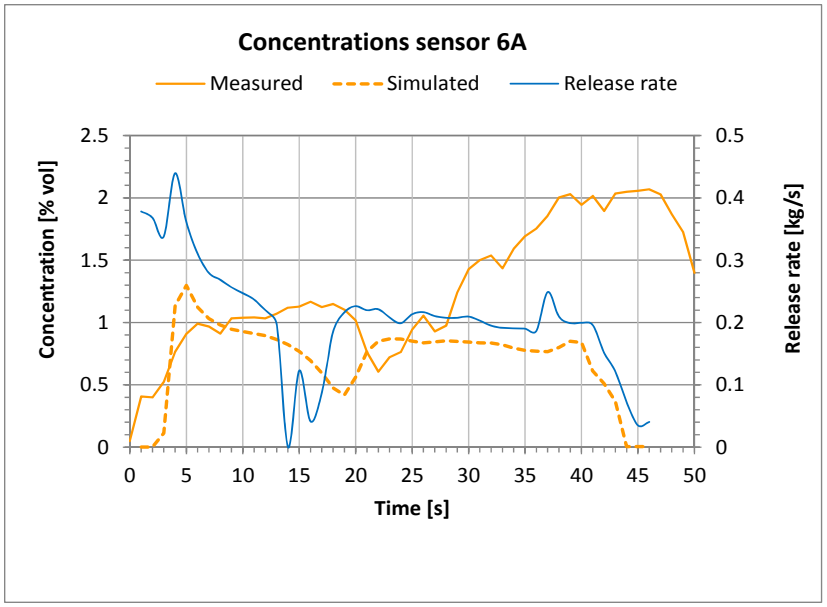

Figure 7

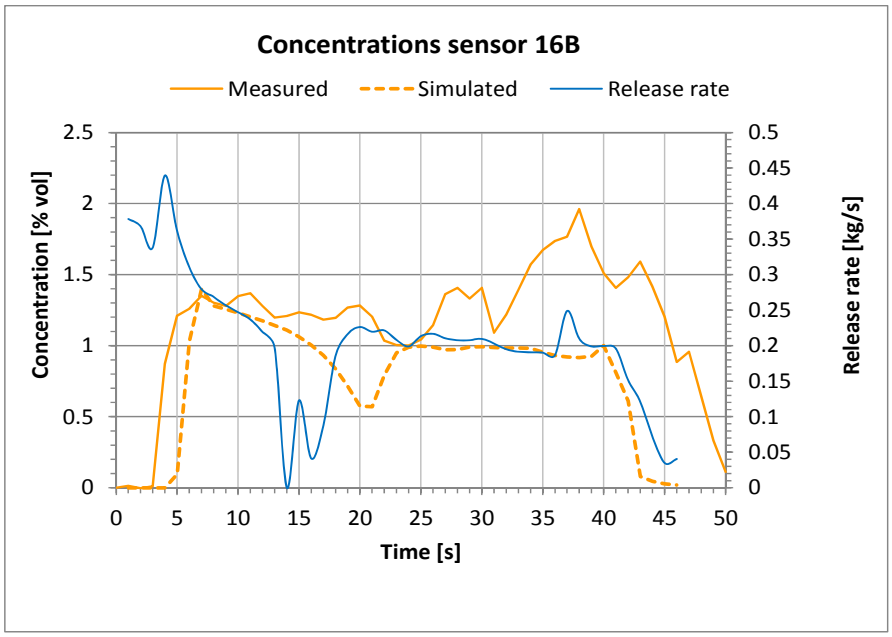

Figure 8

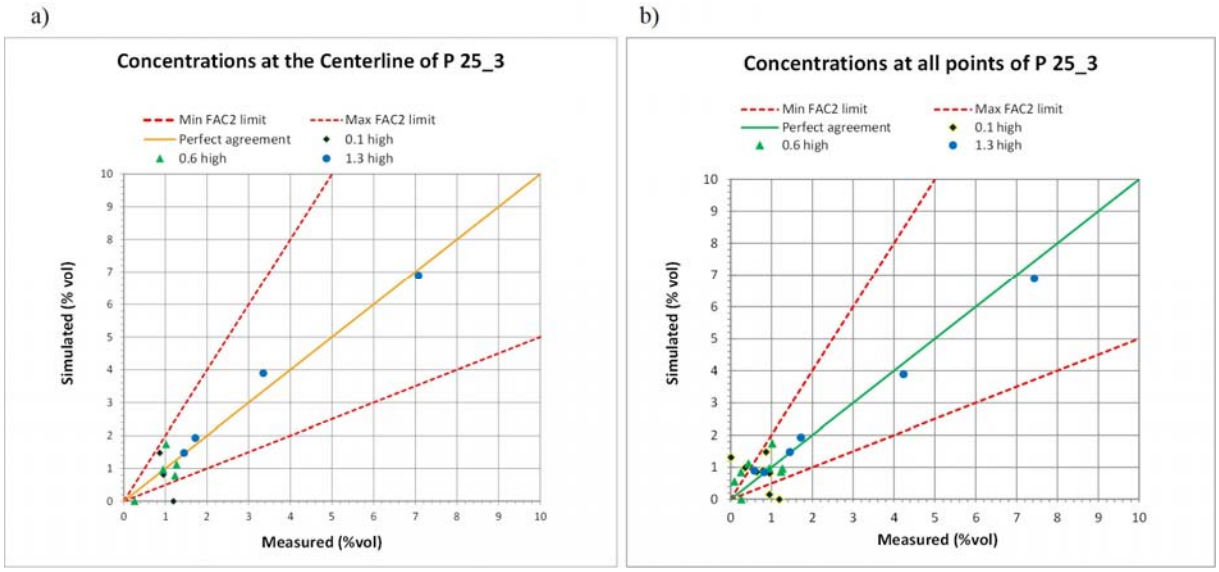

Figure 9

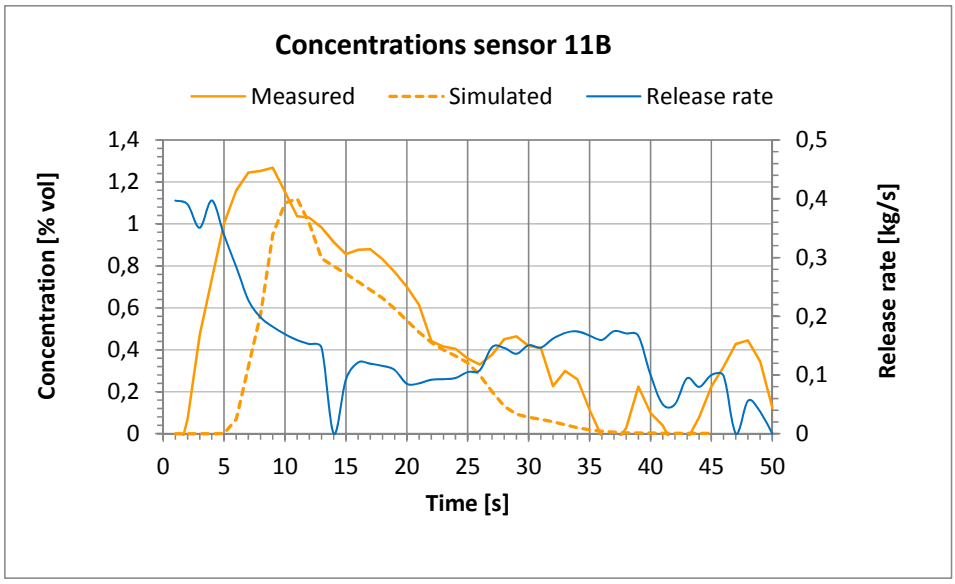

Figure 10

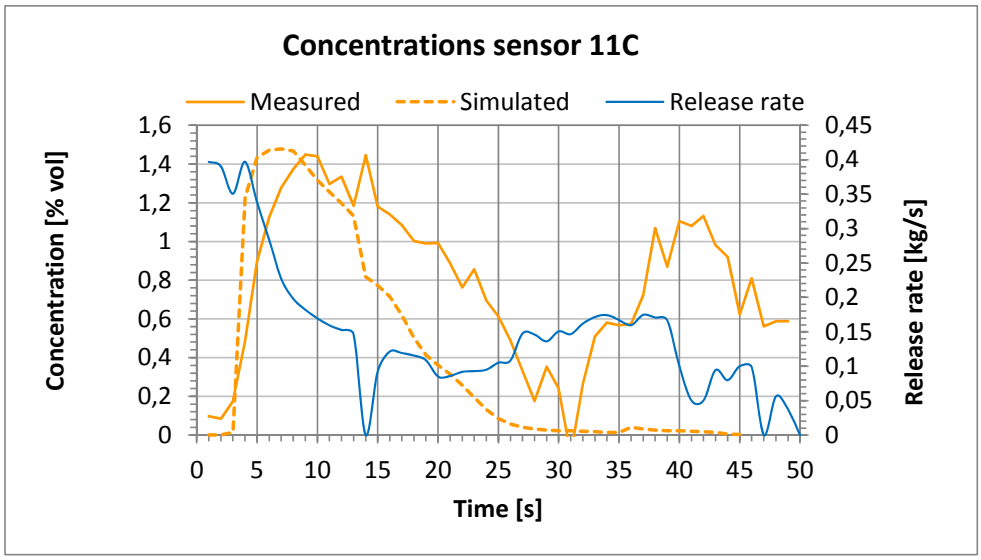

Figure 11

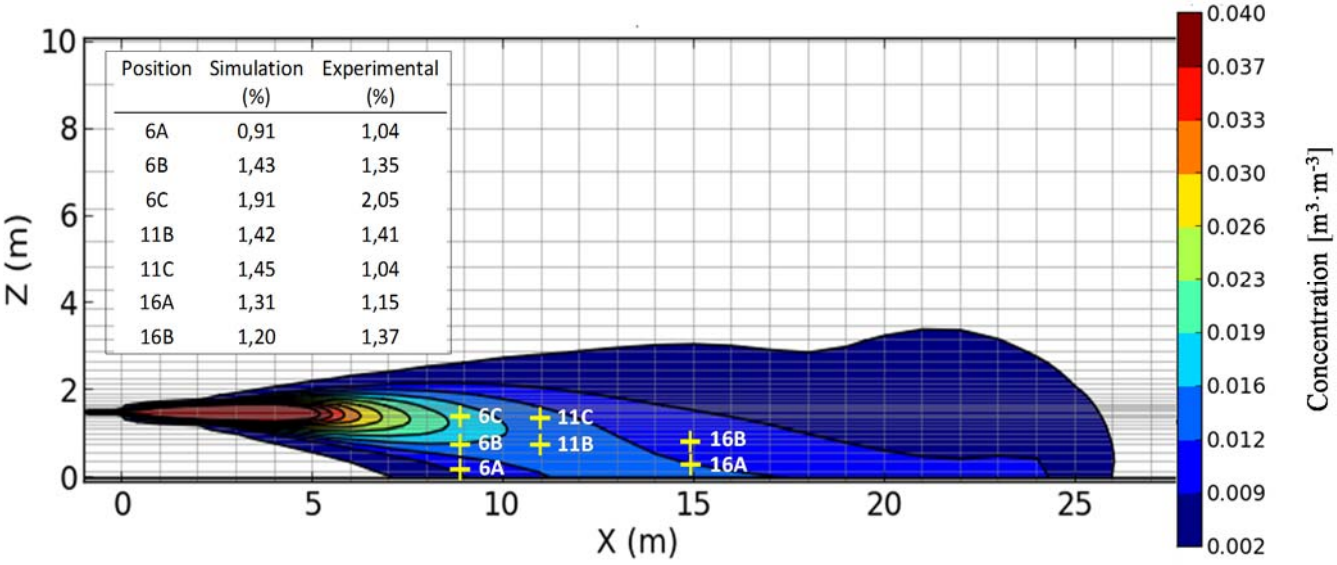
Position | Simulation (%) | Experimental (%)
6A | 0,91 | 1,04
6B | 1,43 | 1,35
6C | 1,91 | 2,05
11B | 1,42 | 1,41
11C | 1,45 | 1,04
16A | 1,31 | 1,15
16B | 1,20 | 1,37
6C
6B
6A
11C
11B
16B
16A
Z (m)
X (m)
Concentration [m³·m⁻³]
0.040
0.037
0.033
0.030
0.026
0.023
0.019
0.016
0.012
0.009
0.002

Figure 12

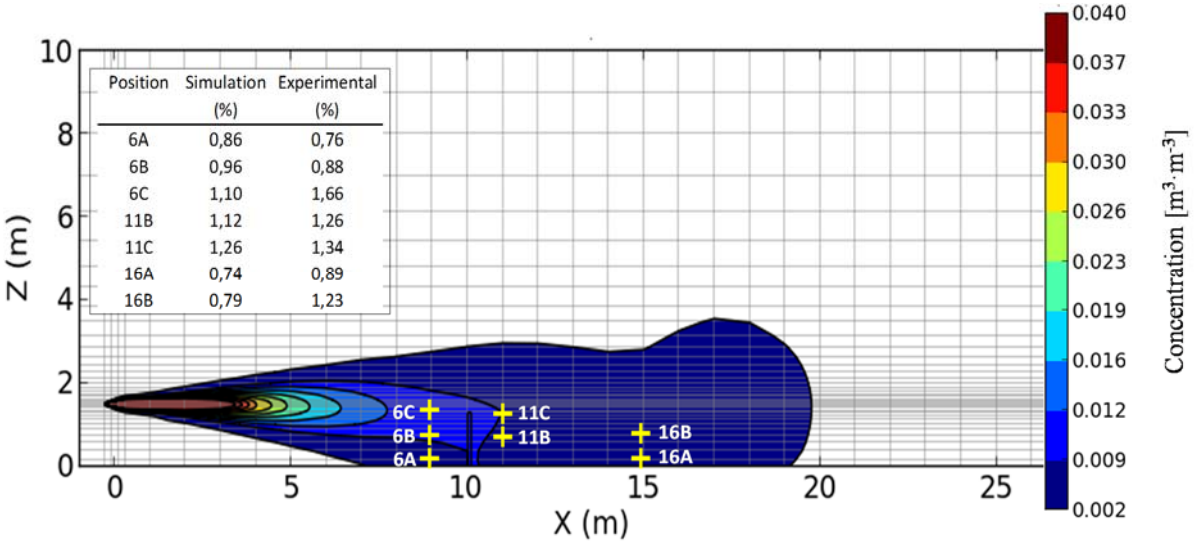
Position | Simulation (%) | Experimental (%)
6A | 0,86 | 0,76
6B | 0,96 | 0,88
6C | 1,10 | 1,66
11B | 1,12 | 1,26
11C | 1,26 | 1,34
16A | 0,74 | 0,89
16B | 0,79 | 1,23
6C
6B
6A
11C
11B
16B
16A
Z (m)
X (m)
Concentration [m³·m⁻³]
0.040
0.037
0.033
0.030
0.026
0.023
0.019
0.016
0.012
0.009
0.002

ANNEX A

In this Annex concentration values and release rates of trials P25_2 and P25_3 are presented. The concentration measures are presented as function of time for each sensor placed in the field tests; the trials presented here were carried out in a very cloudy day with scattered showers; the rain before the trials created a more stable atmosphere; however, several sensors did not work well due to accumulated water over the sensor output. In the following tables only the measured values corresponding to the sensor that worked well during the trials are presented. The concentrations and release rates provided are both 1 s-averaged.

Table A 1 shows the discharge rate of trial P25_2; Table A 2 and Table A 3 show the concentrations for each active sensor of trial P25_2; Table A 4 shows the discharge rate of trial P25_3; Table A 5 and Table A 6 present the concentrations for each active sensor of trial P25_3.

Table A 1- Release rate of trial P25_2.

Time [s]	Temperature at outlet orifice [ºC]	Pressure at outlet orifice [hPa]	Release rate [kg.s^{-1}]
1	4.68	590	0.38
2	-10.94	1070	0.37
3	-11.97	740	0.34
4	-7.85	480	0.44
5	-1.77	320	0.36
6	2.17	230	0.31
7	4.02	190	0.28
8	4.40	170	0.27
9	3.99	160	0.26
10	3.06	140	0.25
11	2.08	130	0.24
12	0.77	110	0.22
13	-1.92	90	0.20
14	-4.98	0	0.00
15	-10.52	40	0.12
16	-15.03	10	0.04
17	-25.14	30	0.09
18	-26.98	70	0.19
19	-27.56	100	0.22
20	-27.90	110	0.23
21	-27.93	100	0.22
22	-27.91	100	0.22
23	-27.92	90	0.21
24	-27.95	80	0.20
25	-27.76	90	0.21
26	-28.01	100	0.22
27	-27.96	90	0.21
28	-27.99	90	0.21
29	-28.02	90	0.21
30	-28.07	90	0.21
31	-28.09	80	0.20
32	-28.05	80	0.19
33	-28.07	80	0.19
34	-28.10	70	0.19
35	-28.13	70	0.19
36	-28.09	70	0.19
37	-28.05	130	0.25
38	-28.07	90	0.21
39	-28.12	80	0.20
40	-28.15	80	0.20

Table A 2 -Concentrations of trial P25_2 (sensors 1A to 7B).

Sensor	1A	1B	1C	3B	3C	4A	4B	5A	5B	5C	6A	6B	6C	7A	7B
y [m]	0.0	0.0	0.0	0.0	0.0	-2.0	-2.0	2.0	2.0	2.0	0.0	0.0	0.0	-2.0	-2.0
x [m]	2.0	2.0	2.0	5.0	5.0	5.0	5.0	9.0	9.0	9.0	9.0	9.0	9.0	9.0	9.0
z [m]	0.1	0.6	1.3	0.6	1.3	0.1	0.6	0.1	0.6	1.3	0.1	0.6	1.3	0.1	0.6
Time [s]															
1	0.05	0.09	0.44	0.07	0.38	0.01	0.10	0.00	0.06	0.14	0.41	0.29	0.30	0.45	0.44
2	0.34	0.18	2.16	0.14	1.05	0.06	0.17	0.00	0.08	0.18	0.40	0.56	0.62	0.35	0.34
3	0.51	0.24	3.41	0.30	2.07	0.07	0.05	0.00	0.08	0.18	0.52	0.86	1.10	0.32	0.32
4	0.46	0.34	3.81	0.43	2.58	0.09	0.07	0.00	0.06	0.13	0.76	1.12	1.71	0.27	0.30
5	0.34	0.25	4.06	0.44	2.96	0.12	0.07	0.00	0.11	0.12	0.91	1.33	1.95	0.16	0.25
6	0.49	0.16	4.23	0.53	3.13	0.13	0.07	0.07	0.22	0.16	0.99	1.44	1.93	0.13	0.18
7	0.49	0.02	4.47	0.58	3.31	0.20	0.06	0.14	0.24	0.19	0.97	1.41	2.01	0.28	0.11
8	0.52	0.00	4.58	0.48	3.39	0.22	0.06	0.13	0.13	0.23	0.91	1.34	2.04	0.36	0.00
9	0.48	0.00	4.53	0.50	3.43	0.21	0.05	0.08	0.17	0.33	1.03	1.40	2.10	0.54	0.06
10	0.39	0.02	4.62	0.51	3.47	0.20	0.05	0.16	0.25	0.31	1.04	1.40	2.10	0.27	0.22
11	0.31	0.08	4.44	0.51	3.46	0.15	0.04	0.11	0.19	0.24	1.04	1.35	2.05	0.19	0.32
12	0.27	0.12	4.51	0.54	3.41	0.10	0.05	0.00	0.07	0.13	1.03	1.41	2.01	0.13	0.22
13	0.05	0.19	4.53	0.57	3.31	0.20	0.06	0.00	0.00	0.08	1.07	1.51	2.01	0.04	0.04
14	0.00	0.08	4.62	0.50	3.28	0.25	0.06	0.00	0.00	0.17	1.12	1.48	2.04	0.06	0.05
15	0.00	0.00	4.55	0.36	3.18	0.21	0.06	0.00	0.06	0.27	1.13	1.51	1.94	0.19	0.17
16	0.00	0.00	4.50	0.54	3.24	0.11	0.06	0.00	0.15	0.25	1.17	1.55	1.96	0.21	0.11
17	0.00	0.00	4.47	0.50	3.16	0.00	0.06	0.00	0.12	0.27	1.12	1.56	1.98	0.29	0.17
18	0.00	0.01	4.24	0.30	3.20	0.00	0.05	0.09	0.10	0.16	1.15	1.57	1.98	0.12	0.36
19	0.00	0.05	4.28	0.34	3.29	0.00	0.04	0.15	0.06	0.14	1.10	1.51	1.97	0.20	0.54
20	0.00	0.05	4.54	0.36	3.34	0.00	0.03	0.12	0.03	0.11	1.02	1.36	1.97	0.33	0.49
21	0.03	0.15	5.21	0.33	3.35	0.00	0.03	0.00	0.01	0.10	0.76	1.31	1.98	0.35	0.35
22	0.37	0.26	5.24	0.34	3.47	0.00	0.03	0.00	0.04	0.15	0.61	1.45	2.00	0.29	0.15
23	0.44	0.27	5.28	0.49	3.54	0.00	0.03	0.00	0.06	0.20	0.72	1.53	2.04	0.41	0.10

Sensor	1A	1B	1C	3B	3C	4A	4B	5A	5B	5C	6A	6B	6C	7A	7B
y [m]	0.0	0.0	0.0	0.0	0.0	-2.0	-2.0	2.0	2.0	2.0	0.0	0.0	0.0	-2.0	-2.0
x [m]	2.0	2.0	2.0	5.0	5.0	5.0	5.0	9.0	9.0	9.0	9.0	9.0	9.0	9.0	9.0
z [m]	0.1	0.6	1.3	0.6	1.3	0.1	0.6	0.1	0.6	1.3	0.1	0.6	1.3	0.1	0.6
24	0.32	0.25	5.41	0.68	3.66	0.01	0.03	0.00	0.06	0.18	0.76	1.62	2.12	0.51	0.22
25	0.26	0.17	5.56	0.41	3.79	0.02	0.02	0.00	0.06	0.17	0.94	1.63	2.22	0.65	0.52
26	0.26	0.09	5.66	0.28	3.93	0.08	0.02	0.00	0.09	0.34	1.05	1.68	2.29	0.57	0.59
27	0.25	0.05	5.77	0.20	4.08	0.13	0.01	0.00	0.20	0.33	0.93	1.68	2.35	0.59	0.55
28	0.17	0.06	6.10	0.48	4.21	0.07	0.01	0.00	0.14	0.21	0.97	1.76	2.42	0.65	0.54
29	0.20	0.14	6.18	0.78	4.24	0.00	0.00	0.00	0.08	0.14	1.24	1.90	2.51	0.61	0.56
30	0.37	0.14	6.30	0.77	4.34	0.00	0.00	0.00	0.05	0.11	1.43	2.01	2.59	0.64	0.54
31	2.25	0.07	6.51	0.73	4.40	0.00	0.00	0.00	0.02	0.10	1.50	2.02	2.63	0.78	0.54
32	1.10	0.08	6.52	0.72	4.49	0.00	0.00	0.00	0.02	0.08	1.54	2.07	2.70	1.00	0.65
33	0.44	0.09	6.39	0.68	4.51	0.00	0.00	0.01	0.02	0.05	1.43	2.20	2.73	0.95	0.64
34	0.36	0.11	6.31	0.74	4.60	0.00	0.00	0.10	0.03	0.08	1.59	2.29	2.77	0.81	0.54
35	0.32	0.14	6.41	0.89	4.70	0.00	0.00	0.24	0.07	0.05	1.69	2.39	2.84	0.87	0.51
36	0.29	0.13	6.59	1.12	4.72	0.00	0.00	0.30	0.10	0.06	1.75	2.44	2.88	0.77	0.51
37	0.36	0.08	6.73	1.19	4.75	0.00	0.00	0.03	0.08	0.11	1.86	2.48	2.85	0.86	0.46
38	0.36	0.15	6.91	1.05	4.80	0.00	0.00	0.02	0.05	0.11	2.00	2.51	2.77	0.70	0.39
39	0.29	0.15	6.91	1.00	4.74	0.03	0.00	0.00	0.05	0.09	2.03	2.55	2.68	0.38	0.30
40	0.25	0.09	7.06	1.23	4.84	0.05	0.00	0.00	0.06	0.07	1.95	2.43	2.59	0.33	0.24
41	0.25	0.15	7.43	1.20	4.94	0.06	0.00	0.02	0.01	0.01	2.01	2.43	2.55	0.42	0.27
42	0.27	0.21	7.42	1.15	4.90	0.10	0.00	0.00	0.00	0.00	1.90	2.47	2.47	0.68	0.35
43	1.56	0.18	7.7.43	0.86	5.19	0.13	0.00	0.00	0.00	0.05	2.03	2.44	2.33	0.67	0.23
44	2.36	0.19	7.40	0.78	5.13	0.10	0.00	0.18	0.00	0.04	2.05	2.41	2.19	0.57	0.21
45	0.77	0.20	7.35	0.85	4.57	0.06	0.00	0.18	0.00	0.03	2.06	2.28	2.09	0.49	0.31
46	0.33	0.18	4.32	0.82	3.81	0.06	0.00	0.14	0.23	0.07	2.07	2.15	1.79	0.36	0.39
47	0.24	0.12	2.08	0.67	2.50	0.15	0.00	0.16	0.36	0.13	2.03	2.05	1.59	0.24	0.36

Sensor	1A	1B	1C	3B	3C	4A	4B	5A	5B	5C	6A	6B	6C	7A	7B
y [m]	0.0	0.0	0.0	0.0	0.0	-2.0	-2.0	2.0	2.0	2.0	0.0	0.0	0.0	-2.0	-2.0
x [m]	2.0	2.0	2.0	5.0	5.0	5.0	5.0	9.0	9.0	9.0	9.0	9.0	9.0	9.0	9.0
z [m]	0.1	0.6	1.3	0.6	1.3	0.1	0.6	0.1	0.6	1.3	0.1	0.6	1.3	0.1	0.6
48	0.10	0.12	0.56	0.51	1.79	0.09	0.00	0.28	0.42	0.20	1.87	1.91	1.22	0.11	0.35
49	0.27	0.13	0.00	0.13	1.08	0.10	0.00	0.39	0.48	0.42	1.73	1.57	0.79	0.05	0.29
50	0.40	0.11	0.00	0.00	0.67	0.08	0.00	0.40	0.58	0.37	1.40	1.23	0.54	0.07	0.25
Minimum	0.00	0.00	0.44	0.00	0.38	0.00	0.00	0.00	0.00	0.01	0.40	0.29	0.30	0.04	0.00
Maximum	2.36	0.34	7.43	1.23	5.19	0.25	0.17	0.40	0.58	0.42	2.07	2.55	2.88	1.00	0.65
Values averaged by 1 s															

Table A 3 -Concentrations of trial P25_2 (sensors 7C to16B)

Sensor	7C	9A	10A	10B	10C	11B	11C	12A	12C	13A	15A	15B	16A	16B
y [m]	-2.0	-3.0	2.0	2.0	2.0	0.0	0.0	-2.0	-2.0	2.0	0.0	0.0	-2.0	-2.0
x [m]	9.0	10.0	11.0	11.0	11.0	11.0	11.0	11.0	11.0	13.0	15.0	15.0	13.0	13.0
z [m]	1.3	0.1	0.1	0.6	1.3	0.6	1.3	0.1	1.3	0.6	0.1	0.6	0.1	0.6
Time [s]														
1	0.08	0.00	0.13	0.18	0.15	0.13	0.00	0.02	0.00	0.00	0.00	0.00	0.08	0.01
2	0.07	0.00	0.00	0.11	0.20	0.27	0.16	0.05	0.00	0.00	0.00	0.04	0.11	0.00
3	0.05	0.01	0.00	0.19	0.25	0.76	0.62	0.05	0.00	0.00	0.04	0.05	0.21	0.01
4	0.02	0.07	0.36	0.32	0.31	1.18	2.85	0.50	0.18	0.00	0.63	0.17	0.55	0.87
5	0.00	0.00	0.29	0.36	0.43	1.36	0.00	0.36	0.39	0.07	0.66	0.17	0.91	1.21
6	0.03	0.00	0.44	0.41	0.39	1.53	0.17	0.23	0.42	0.06	0.51	0.26	1.16	1.26
7	0.00	0.00	0.76	0.39	0.49	1.50	0.98	0.26	0.30	0.23	0.69	0.37	1.24	1.35
8	0.00	0.00	0.82	0.44	0.57	1.49	1.18	0.18	0.24	0.39	0.81	0.40	1.09	1.30
9	0.00	0.00	0.68	0.34	0.44	1.48	1.40	0.06	0.19	0.47	0.67	0.42	1.09	1.28

10	0.02	0.00	0.37	0.32	0.42	1.45	1.40	0.10	0.03	0.49	0.59	0.28	1.15	1.35
11	0.00	0.00	0.01	0.30	0.43	1.41	1.04	0.10	0.00	0.37	0.52	0.27	1.15	1.37
12	0.00	0.00	0.03	0.30	0.36	1.36	1.25	0.00	0.00	0.22	0.63	0.20	1.15	1.28
13	0.00	0.00	0.00	0.27	0.25	1.45	1.75	0.00	0.00	0.16	0.57	0.02	1.05	1.20
14	0.00	0.00	0.00	0.17	0.26	1.46	1.44	0.00	0.00	0.03	0.25	0.00	0.99	1.21
15	0.00	0.00	0.00	0.15	0.39	1.45	1.33	0.00	0.00	0.00	0.25	0.00	1.08	1.24
16	0.00	0.00	0.00	0.36	0.34	1.42	1.71	0.00	0.00	0.00	0.23	0.00	1.08	1.22
17	0.04	0.00	0.00	0.42	0.51	1.44	1.80	0.00	0.00	0.01	0.18	0.05	1.06	1.18
18	0.21	0.00	0.05	0.26	0.47	1.50	1.49	0.05	0.00	0.02	0.47	0.20	1.11	1.20
19	0.25	0.00	0.00	0.14	0.32	1.41	1.54	0.03	0.00	0.01	0.67	0.44	1.17	1.27
20	0.20	0.00	0.00	0.06	0.19	1.06	1.77	0.00	0.10	0.03	0.65	0.54	1.11	1.28
21	0.14	0.00	0.00	0.04	0.26	1.03	1.47	0.01	0.17	0.00	0.98	0.48	1.07	1.20
22	0.07	0.00	0.00	0.08	0.53	1.11	1.46	0.20	0.18	0.00	0.89	0.49	0.89	1.04
23	0.04	0.00	0.00	0.12	0.43	1.18	1.56	0.40	0.14	0.00	0.93	0.47	0.68	1.00
24	0.01	0.00	0.10	0.27	0.49	1.30	1.59	0.41	0.00	0.00	1.00	0.49	0.86	1.00
25	0.02	0.00	0.06	0.43	0.36	1.42	1.68	0.38	0.00	0.00	0.93	0.66	0.97	1.04
26	0.05	0.00	0.22	0.52	0.42	1.53	1.78	0.61	0.04	0.00	0.78	0.71	1.10	1.14
27	0.09	0.00	0.08	0.44	0.50	1.56	1.79	0.52	0.18	0.00	0.93	0.79	1.19	1.36
28	0.11	0.00	0.24	0.41	0.52	1.60	1.81	0.80	0.34	0.00	0.82	0.56	1.21	1.41
29	0.12	0.00	0.14	0.40	0.48	1.69	1.78	0.69	0.33	0.00	0.89	0.44	1.25	1.33
30	0.24	0.00	0.01	0.33	0.35	1.83	2.15	0.71	0.20	0.00	0.62	0.26	1.28	1.41
31	0.45	0.00	0.00	0.20	0.21	1.88	2.09	0.68	0.03	0.00	0.72	0.25	1.42	1.09
32	0.42	0.00	0.00	0.21	0.17	1.97	1.94	0.61	0.00	0.00	0.94	0.37	1.57	1.22
33	0.33	0.00	0.00	0.14	0.13	2.04	1.93	0.56	0.00	0.06	1.12	0.51	1.74	1.39
34	0.28	0.00	0.00	0.27	0.16	2.08	2.01	0.59	0.00	0.13	1.18	0.70	1.88	1.57
35	0.25	0.00	0.43	0.63	0.15	2.15	2.02	0.65	0.00	0.00	1.28	0.72	1.94	1.67
36	0.04	0.00	0.75	0.59	0.05	2.36	1.91	0.74	0.00	0.00	1.26	0.49	1.92	1.74
37	0.00	0.00	0.87	0.37	0.00	2.38	2.28	0.66	0.00	0.06	1.45	0.70	1.97	1.77

38	0.00	0.00	0.86	0.29	0.00	2.33	2.12	0.81	0.00	0.35	1.33	0.85	2.06	1.96
39	0.00	0.00	0.80	0.31	0.05	2.31	1.90	1.00	0.00	0.38	1.43	0.93	2.07	1.70
40	0.00	0.00	0.81	0.46	0.00	2.25	2.00	1.13	0.00	0.54	1.53	0.99	1.99	1.51
41	0.00	0.00	0.89	0.71	0.03	2.29	1.92	1.21	0.00	0.87	1.44	0.96	1.92	1.41
42	0.00	0.00	0.98	0.50	0.07	2.22	1.60	1.17	0.00	0.90	1.29	0.87	1.81	1.48
43	0.01	0.00	1.00	0.55	0.22	2.03	1.38	1.03	0.00	1.13	1.25	0.87	1.77	1.59
44	0.08	0.00	1.29	0.77	0.34	1.90	1.24	0.95	0.00	1.30	1.36	1.06	1.76	1.42
45	0.11	0.00	1.04	0.75	0.46	1.87	1.25	1.03	0.00	1.34	1.46	0.95	1.54	1.20
46	0.08	0.00	0.85	0.68	0.53	1.86	1.16	0.96	0.00	1.29	1.67	1.02	1.51	0.89
47	0.06	0.00	0.87	0.77	0.68	1.67	0.92	0.83	0.00	1.31	1.55	0.87	1.62	0.96
48	0.08	0.00	1.05	0.78	0.53	1.42	0.55	0.74	0.00	1.32	1.46	0.78	1.34	0.64
49	0.00	0.00	1.12	1.11	0.64	1.09	0.35	0.61	0.00	1.44	1.27	0.71	1.04	0.33
50	0.00	0.00	0.93	0.72	0.57	0.87	0.19	0.45	0.08	1.40	1.01	0.18	0.90	0.11
Minimum	0.00	0.00	0.00	0.04	0.00	0.13	0.00	0.00	0.00	0.00	0.00	0.00	0.08	0.00
Maximum	0.45	0.07	1.29	1.11	0.68	2.38	2.85	1.21	0.42	1.44	1.67	1.06	2.07	1.96
Values averaged by 1 s														

Table A 4 - Release rate of trial P25_3

Time [s]	Temperature at outlet orifice [ºC]	Pressure at outlet orifice [hPa]	Release rate [kg.s^{-1}]
1	10.26	740	0.40
2	-12.66	1330	0.39
3	-11.85	880	0.35
4	-7.46	380	0.40
5	-2.45	240	0.34
6	1.84	170	0.28
7	3.23	110	0.23
8	4.44	90	0.20
9	5.07	80	0.18
10	5.46	70	0.17
11	5.58	60	0.16
12	5.52	50	0.15
13	5.17	50	0.15
14	4.75	0	0.00
15	4.19	40	0.09
16	3.23	30	0.12
17	2.49	30	0.12
18	0.93	30	0.12
19	-0.89	30	0.11
20	-4.10	20	0.09
21	-10.30	20	0.09
22	-14.08	20	0.09
23	-22.00	20	0.09
24	-26.70	20	0.09
25	-27.21	20	0.11
26	-27.86	20	0.11
27	-28.13	50	0.15
28	-28.35	40	0.15
29	-28.41	40	0.14
30	-28.34	50	0.15
31	-28.30	40	0.15
32	-28.23	50	0.16
33	-28.18	60	0.17
34	-28.24	60	0.17
35	-28.30	60	0.17
36	-28.32	50	0.16
37	-28.16	60	0.17
38	-28.16	60	0.17
39	-28.26	60	0.17
40	-28.30	80	0.17

Table A 5 - Concentrations of trial P25_3(sensors 1A to 6C).

Sensor	1A	1B	1C	3B	3C	4A	4B	5A	5B	5C	6A	6B	6C
y [m]	0.0	0.0	0.0	0.0	0.0	-2.0	-2.0	2.0	2.0	2.0	0.0	0.0	0.0
x [m]	2.0	2.0	2.0	5.0	5.0	5.0	5.0	9.0	9.0	9.0	9.0	9.0	9.0
z [m]	0.1	0.6	1.3	0.6	1.3	0.1	0.6	0.1	0.6	1.3	0.1	0.6	1.3
Time [s]													
1	0.19	0.00	0.21	0.05	0.00	0.45	0.00	0.00	0.00	0.00	0.00	0.00	0.00
2	0.06	0.00	1.64	0.03	0.86	0.47	0.00	0.00	0.00	0.00	0.00	0.00	0.25
3	0.05	0.00	2.76	0.15	1.51	0.62	0.00	0.00	0.00	0.00	0.16	0.22	0.76
4	0.00	0.00	3.36	0.44	2.21	0.69	0.00	0.00	0.00	0.00	0.35	0.63	1.20
5	0.00	0.00	3.72	0.41	2.63	0.65	0.00	0.00	0.00	0.00	0.80	0.91	1.56
6	0.08	0.05	3.86	0.59	2.91	0.69	0.00	0.00	0.00	0.00	0.86	0.92	1.69
7	0.07	0.19	3.80	0.83	3.04	0.67	0.00	0.00	0.00	0.00	0.79	0.90	1.72
8	0.16	0.26	4.19	0.93	3.12	0.80	0.00	0.04	0.00	0.00	0.76	0.89	1.69
9	0.25	0.15	4.21	0.94	3.12	0.89	0.00	0.23	0.00	0.00	0.73	0.88	1.65
10	0.19	0.00	4.31	0.75	3.04	0.94	0.00	0.33	0.00	0.00	0.65	0.92	1.54
11	0.00	0.00	4.39	0.59	2.96	0.95	0.00	0.21	0.00	0.00	0.82	1.02	1.58
12	0.00	0.00	4.33	0.52	2.92	0.77	0.00	0.16	0.00	0.00	0.86	0.89	1.48
13	0.00	0.00	4.20	0.61	2.86	0.52	0.00	0.30	0.00	0.00	0.76	0.69	1.34
14	0.00	0.06	3.76	0.61	2.75	0.28	0.00	0.45	0.02	0.00	0.68	0.58	1.19
15	0.33	0.06	3.65	0.56	2.64	0.28	0.00	0.40	0.09	0.00	0.63	0.56	1.08
16	0.36	0.15	3.88	0.44	2.52	0.31	0.00	0.79	0.00	0.00	0.50	0.47	0.94
17	0.00	0.26	3.75	0.29	2.45	0.17	0.00	0.53	0.00	0.00	0.40	0.36	0.74
18	0.00	0.12	3.65	0.24	2.44	0.00	0.00	0.03	0.00	0.00	0.44	0.40	0.70
19	0.00	0.01	3.58	0.33	2.38	0.00	0.00	0.00	0.00	0.00	0.27	0.36	0.63

Sensor	1A	1B	1C	3B	3C	4A	4B	5A	5B	5C	6A	6B	6C
y [m]	**0.0**	**0.0**	**0.0**	**0.0**	**0.0**	**-2.0**	**-2.0**	**2.0**	**2.0**	**2.0**	**0.0**	**0.0**	**0.0**
x [m]	**2.0**	**2.0**	**2.0**	**5.0**	**5.0**	**5.0**	**5.0**	**9.0**	**9.0**	**9.0**	**9.0**	**9.0**	**9.0**
z [m]	**0.1**	**0.6**	**1.3**	**0.6**	**1.3**	**0.1**	**0.6**	**0.1**	**0.6**	**1.3**	**0.1**	**0.6**	**1.3**
20	0.00	0.00	3.50	0.40	2.32	0.15	0.00	0.00	0.00	0.00	0.16	0.27	0.64
21	0.00	0.00	3.27	0.31	1.99	0.35	0.00	0.00	0.00	0.00	0.05	0.16	0.51
22	0.00	0.00	3.49	0.25	1.91	0.23	0.00	0.63	0.00	0.00	0.03	0.00	0.37
23	0.00	0.00	3.79	0.29	2.01	0.05	0.00	0.73	0.00	0.00	0.12	0.00	0.34
24	0.00	0.00	3.64	0.31	2.04	0.26	0.00	0.47	0.00	0.00	0.11	0.06	0.36
25	0.00	0.00	3.57	0.47	2.04	0.33	0.00	0.49	0.00	0.00	0.09	0.04	0.43
26	0.00	0.00	3.61	0.63	2.09	0.47	0.00	0.41	0.00	0.00	0.09	0.02	0.50
27	0.01	0.00	3.73	0.43	2.26	0.51	0.00	0.25	0.00	0.00	0.00	0.02	0.46
28	0.07	0.00	3.99	0.41	2.26	0.65	0.00	0.00	0.00	0.00	0.00	0.10	0.45
29	0.23	0.00	4.46	0.45	2.23	0.75	0.00	0.00	0.00	0.00	0.00	0.16	0.49
30	0.45	0.02	4.48	0.55	2.26	0.72	0.00	0.00	0.00	0.00	0.11	0.24	0.63
31	0.44	0.06	4.56	0.61	2.26	0.65	0.00	0.00	0.00	0.00	0.11	0.31	0.71
32	0.52	0.02	4.82	0.76	2.23	0.65	0.00	0.00	0.00	0.00	0.19	0.31	0.67
33	0.51	0.21	5.00	0.92	2.30	0.73	0.00	0.00	0.00	0.00	0.41	0.28	0.62
34	0.61	0.25	4.93	0.79	2.45	0.46	0.00	0.00	0.00	0.00	0.48	0.26	0.29
35	0.40	0.26	5.07	0.65	2.57	0.00	0.00	0.00	0.00	0.00	0.41	0.28	0.10
36	0.20	0.17	5.12	0.80	2.70	0.00	0.00	0.00	0.00	0.00	0.51	0.31	0.26
37	0.22	0.10	5.33	0.71	2.74	0.00	0.00	0.00	0.00	0.00	0.36	0.34	0.28
38	0.36	0.03	5.89	0.61	2.85	0.00	0.00	0.00	0.00	0.00	0.41	0.26	0.24
39	0.68	0.03	6.57	0.58	3.03	0.00	0.00	0.00	0.00	0.00	0.46	0.13	0.14
40	0.66	0.14	6.80	0.35	3.16	0.07	0.00	0.00	0.00	0.00	0.44	0.00	0.00
41	1.19	0.10	7.08	0.25	3.35	0.60	0.00	0.00	0.00	0.00	0.41	0.00	0.00
42	0.68	0.03	6.57	0.64	3.55	0.83	0.00	0.00	0.00	0.00	0.47	0.00	0.00
43	0.68	0.06	6.63	0.68	3.66	0.92	0.03	0.00	0.00	0.00	0.45	0.24	0.23

Sensor	1A	1B	1C	3B	3C	4A	4B	5A	5B	5C	6A	6B	6C
y [m]	**0.0**	**0.0**	**0.0**	**0.0**	**0.0**	**-2.0**	**-2.0**	**2.0**	**2.0**	**2.0**	**0.0**	**0.0**	**0.0**
x [m]	**2.0**	**2.0**	**2.0**	**5.0**	**5.0**	**5.0**	**5.0**	**9.0**	**9.0**	**9.0**	**9.0**	**9.0**	**9.0**
z [m]	**0.1**	**0.6**	**1.3**	**0.6**	**1.3**	**0.1**	**0.6**	**0.1**	**0.6**	**1.3**	**0.1**	**0.6**	**1.3**
44	0.67	0.09	6.69	0.37	3.79	1.00	0.08	0.00	0.00	0.00	0.56	0.50	0.55
45	0.66	0.11	6.75	0.28	0.14	0.91	0.05	0.00	0.00	0.00	0.77	0.75	0.81
46	0.66	0.14	6.80	0.93	4.03	0.77	0.05	0.15	0.00	0.00	1.06	1.04	0.70
47	0.79	0.13	6.80	1.32	4.23	0.54	0.07	0.04	0.00	0.00	1.35	0.83	0.45
48	0.93	0.12	6.89	1.11	4.23	0.42	0.37	0.51	0.00	0.00	1.31	0.66	0.21
49	1.06	0.11	6.99	0.65	3.44	0.07	0.18	0.18	0.00	0.00	1.07	0.59	0.05
50	1.19	0.10	7.08	0.14	2.89	0.02	0.17	0.00	0.00	0.00	1.00	0.25	0.00
Minimum	0.00	0.00	0.21	0.03	0.00	0.00	0.00	0.00	0.00	0.00	0.00	0.00	0.00
Maximum	1.19	0.26	7.08	1.32	4.23	1.00	0.37	0.79	0.09	0.00	1.35	1.04	1.72
Values averaged by 1 s													

Table A 6 -Concentrations of trial P25_3 (sensors 7A to 15A)

Sensor	7A	7B	7C	9A	10B	11B	11C	12A	12C	13A	15A	16A	16B
y [m]	**-2.0**	**-2.0**	**-2.0**	**-3.0**	**2.0**	**0.0**	**0.0**	**-2.0**	**-2.0**	**2.0**	**-2.0**	**0.0**	**0.0**
x [m]	**9.0**	**9.0**	**9.0**	**10.0**	**11.0**	**11.0**	**11.0**	**11.0**	**11.0**	**13.0**	**13.0**	**15.0**	**15.0**
z [m]	**0.1**	**0.6**	**1.3**	**0.1**	**0.6**	**0.6**	**1.3**	**0.1**	**1.3**	**0.6**	**0.1**	**0.1**	**0.6**
Time [s]													
1	0.01	0.00	0.00	0.10	0.00	0.00	0.70	0.01	0.38	0.00	0.05	0.00	0.00
2	0.00	0.00	0.00	0.01	0.00	0.07	0.10	0.01	0.06	0.00	0.05	0.00	0.00
3	0.06	0.00	0.11	0.00	0.00	0.47	0.08	0.01	0.00	0.00	0.07	0.00	0.00
4	0.48	0.00	0.18	0.00	0.00	0.73	0.17	0.01	0.00	0.00	0.65	0.33	0.43
5	0.43	0.00	0.18	0.06	0.00	1.00	0.48	0.01	0.00	0.00	0.81	0.65	0.70

Sensor	7A	7B	7C	9A	10B	11B	11C	12A	12C	13A	15A	16A	16B
y [m]	-2.0	-2.0	-2.0	-3.0	2.0	0.0	0.0	-2.0	-2.0	2.0	-2.0	0.0	0.0
x [m]	9.0	9.0	9.0	10.0	11.0	11.0	11.0	11.0	11.0	13.0	13.0	15.0	15.0
z [m]	0.1	0.6	1.3	0.1	0.6	0.6	1.3	0.1	1.3	0.6	0.1	0.1	0.6
6	0.40	0.00	0.39	0.19	0.00	1.16	0.90	0.01	0.01	0.00	1.04	0.80	1.00
7	0.47	0.00	0.51	0.14	0.00	1.25	1.13	0.01	0.05	0.11	1.18	0.95	1.08
8	0.58	0.00	0.56	0.14	0.00	1.25	1.28	0.01	0.11	0.26	1.26	0.84	1.23
9	0.63	0.00	0.71	0.11	0.00	1.27	1.37	0.01	0.30	0.30	1.23	0.92	1.23
10	0.64	0.25	0.72	0.04	0.00	1.15	1.45	0.01	0.14	0.18	1.23	0.87	1.19
11	0.50	0.10	0.71	0.04	0.00	1.04	1.44	0.01	0.12	0.20	1.22	0.74	1.14
12	0.34	0.16	0.60	0.00	0.00	1.03	1.30	0.01	0.20	0.33	1.10	0.63	1.05
13	0.42	0.05	0.55	0.00	0.00	0.98	1.33	0.01	0.23	0.43	0.97	0.57	1.00
14	0.39	0.11	0.55	0.00	0.03	0.91	1.18	0.01	0.19	0.37	0.98	0.53	0.96
15	0.50	0.09	0.63	0.13	0.18	0.86	1.45	0.01	0.21	0.26	0.89	0.35	0.73
16	0.51	0.05	0.65	0.36	0.29	0.88	1.18	0.01	0.21	0.00	0.79	0.38	0.84
17	0.51	0.06	0.60	0.00	0.44	0.88	1.14	0.01	0.17	0.00	0.69	0.38	0.79
18	0.56	0.12	0.48	0.01	0.51	0.83	1.08	0.01	0.28	0.00	0.66	0.28	0.69
19	0.64	0.17	0.51	0.07	0.60	0.77	1.00	0.01	0.25	0.00	0.63	0.26	0.59
20	0.56	0.25	0.42	0.16	0.20	0.70	0.99	0.01	0.58	0.00	0.49	0.20	0.57
21	0.56	0.06	0.35	0.14	0.00	0.61	0.99	0.01	0.32	0.00	0.47	0.00	0.45
22	0.38	0.00	0.26	0.00	0.00	0.44	0.89	0.01	0.09	0.00	0.29	0.00	0.18
23	0.37	0.00	0.15	0.00	0.00	0.42	0.76	0.01	0.00	0.00	0.20	0.00	0.11
24	0.37	0.00	0.08	0.00	0.00	0.41	0.86	0.01	0.00	0.00	0.21	0.00	0.00
25	0.15	0.00	0.14	0.00	0.00	0.36	0.70	0.01	0.00	0.00	0.10	0.00	0.00
26	0.00	0.00	0.26	0.00	0.00	0.33	0.61	0.01	0.00	0.00	0.00	0.00	0.00
27	0.10	0.03	0.21	0.00	0.00	0.38	0.49	0.01	0.00	0.00	0.00	0.00	0.00
28	0.00	0.12	0.21	0.00	0.00	0.45	0.33	0.01	0.00	0.00	0.00	0.00	0.00
29	0.02	0.00	0.07	0.00	0.00	0.46	0.18	0.01	0.14	0.00	0.00	0.00	0.00

Sensor	7A	7B	7C	9A	10B	11B	11C	12A	12C	13A	15A	16A	16B
y [m]	**-2.0**	**-2.0**	**-2.0**	**-3.0**	**2.0**	**0.0**	**0.0**	**-2.0**	**-2.0**	**2.0**	**-2.0**	**0.0**	**0.0**
x [m]	**9.0**	**9.0**	**9.0**	**10.0**	**11.0**	**11.0**	**11.0**	**11.0**	**11.0**	**13.0**	**13.0**	**15.0**	**15.0**
z [m]	**0.1**	**0.6**	**1.3**	**0.1**	**0.6**	**0.6**	**1.3**	**0.1**	**1.3**	**0.6**	**0.1**	**0.1**	**0.6**
30	0.22	0.00	0.00	0.00	0.00	0.42	0.35	0.01	0.24	0.00	0.00	0.00	0.00
31	0.12	0.00	0.06	0.00	0.00	0.41	0.24	0.01	0.16	0.00	0.00	0.00	0.00
32	0.09	0.00	0.21	0.00	0.00	0.23	0.00	0.01	0.00	0.00	0.00	0.00	0.00
33	0.10	0.00	0.25	0.00	0.00	0.30	0.26	0.01	0.00	0.00	0.02	0.00	0.00
34	0.40	0.00	0.14	0.29	0.00	0.26	0.51	0.01	0.00	0.00	0.09	0.00	0.01
35	0.59	0.00	0.19	0.33	0.00	0.11	0.58	0.01	0.13	0.00	0.17	0.00	0.15
36	0.23	0.00	0.05	0.25	0.00	0.00	0.57	0.01	0.03	0.00	0.20	0.00	0.16
37	0.13	0.00	0.35	0.20	0.00	0.00	0.57	0.00	0.00	0.00	0.13	0.00	0.07
38	0.28	0.12	0.54	0.15	0.00	0.03	0.72	0.01	0.00	0.00	0.20	0.00	0.02
39	0.39	0.23	0.57	0.06	0.00	0.22	1.07	0.00	0.00	0.00	0.55	0.00	0.00
40	0.41	0.22	0.55	0.02	0.00	0.10	0.87	0.00	0.00	0.00	0.75	0.00	0.13
41	0.41	0.20	0.53	0.00	0.00	0.04	1.10	0.00	0.00	0.00	0.90	0.00	0.31
42	0.38	0.20	0.53	0.00	0.00	0.00	1.08	0.00	0.00	0.00	0.99	0.00	0.59
43	0.35	0.19	0.57	0.00	0.00	0.00	1.13	0.00	0.00	0.00	1.09	0.00	0.61
44	0.32	0.19	0.62	0.00	0.00	0.08	0.98	0.00	0.00	0.00	1.24	0.00	0.97
45	0.29	0.18	0.67	0.00	0.00	0.22	0.92	0.00	0.00	0.00	1.40	0.00	1.13
46	0.36	0.18	0.71	0.00	0.00	0.32	0.62	0.00	0.00	0.00	1.44	0.00	1.15
47	0.43	0.25	0.82	0.00	0.00	0.43	0.81	0.00	0.00	0.00	1.30	0.00	1.11
48	0.49	0.32	0.93	0.00	0.00	0.44	0.56	0.00	0.00	0.00	1.39	0.00	1.24
49	0.56	0.40	1.04	0.00	0.00	0.35	0.59	0.00	0.00	0.00	1.57	0.00	1.47
50	0.56	0.47	1.15	0.00	0.08	0.12	0.59	0.00	0.00	0.00	1.43	0.00	1.46
Minimum	0.00	0.00	0.00	0.00	0.00	0.00	0.00	0.00	0.00	0.00	0.00	0.00	0.00
Maximum	0.64	0.47	1.15	0.36	0.60	1.27	1.45	0.01	0.58	0.43	1.57	0.95	1.47
Values averaged by 1 s													